PAPER • **OPEN ACCESS**

Effect of substrate thickness on coating roughness Ti/AlTiN during interaction process Parameter

To cite this article: K. J. kadhim and Shakir M. Mousa 2018 *IOP Conf. Ser.: Mater. Sci. Eng.* **454** 012002

Effect of substrate thickness on coating roughness Ti/AlTiN during interaction process Parameter

K. J. kadhim*[,1] , Shakir M. Mousa[2]

[1,2]MAl-Mussaib Technical Institute /Al-Furat Al-Awsat Technical University, 51009 Babylon, Iraq
[1]kamil_jawad35@yahoo.com,[2]Shakir.aljabiri_89@yahoo.com.

Abstract. Ti/TiAlN coatings were deposited on tungsten carbide substrates and consist of the target Ti0.5Al0.5 using sputtering system is one of the main techniques which done be coating substrate. This research aimed is to develop the model a PVD magnetron sputtering process that can predict the relationship between process input parameters and the resulting coating properties and performance. RSM Response Surface Methodology was used, one of the most cost-effective and practical techniques to develop the process model. The influence of substrate thickness on the structural properties of the coatings was investigated and the effect of bias voltage on the microstructure was investigated. The number of crystallite grain size reduced with the increase of the bias voltage then reduce minimum roughness 0.07157 (μm) and became maximum roughness 0.7856 (μm). The crystalline grain size of the coatings increased as the bias voltage was raised from 50 to 75 V, and then decreased with further increase of the bias voltage.

Keywords: Sputtering, surface roughness, PVD, interaction, RSM

1. Introduction

The something observation in a scientific investigation or experiment that is the main goal of thin coating applications is to improve the surface properties of artifacts while maintaining their bulk properties. The application of general rules to particular cases of thin coating on the cutting tools is to improve the cutting tool performance by enhancing the properties of the tool surface. We've used technology to improve relations with the performance of coated cutting tools has been proven and documented such as the application of the coating to cutting tools for different processing techniques, like as continuous cutting and cutting, requires different coating properties, which depend heavily on the parameters of the process under which they are formed. Some published works support this claim [1-6]. As suggest as that coated tool wear performance was 40 times better than the uncoated tools. Aside from prolonging tool life, coated tools can also enable the implementation of Minimum Quantity Lubrication (MQL) and pursuant of dry machining. This can significantly reduce manufacturing costs associated with cutting fluids, which are attributable to 15% of metal machining costs and reduce the environmental impacts associated with the disposal of the cutting fluid [7]. One of the major challenges in surface coating techniques is to develop cost effective coating processes so that an improvement in performance can offset the cost of the coating process [8]. If this can be achieved, end-user adoption of coated cutting tools can be ensured. Unlike cost, having the ability to customize coating properties for machining applications can also provide value-added advantages to the industry. Applications of different parts may require different coating properties as shown in the following studies: D. Kotter, et al., [9] suggested that in the intermittent cutting process, adhesion coating and durability were more important than hardness in determining the cutting instrument performance. Warcholinski, and Gilewicz [10] pointed out that pressure in depositing paint affects the performance of the drilling; Abdul Syukor, et al., [11] indicates that continuous cutting operations such as milling, coating strength and hardness can be related to the performance of the cutting tool. A single approach to addressing both the cost and customization needs of the paint process is through the development of the process model. After developing a process model that can predict the output response of the paint process based on input parameters, the optimization process cannot be performed efficiently. Waste resources such as materials, use of equipment, as well as human resources related to trial and error approaches can be reduced in the experiment. Thanks to the advanced process model, the coating properties required for their excellently specific application can also be expected, through work modelling in thin film operations, which that can be classified into two groups. First, the theoretical methods are mainly based on the Monte Carlo method [12]. Second, the practical way of direct mathematical modelling insomuch as the relationship can be described by a linear function, the approximate function is the first order model; otherwise, it is a second-order model if there is curvature in the relationship [13]. The Monte Carlo Modeling Approach requires intensive investment in the computerization of highly specialized devices and skills; direct mathematical modeling requires highly specialized skills in the process of characterization, coating, substrate and collection. These requirements can be an obstacle for SMEs to implement practical work. The experimental approach in the process of optimization and modeling in PVD processes, as shown in the literature, includes methodologies such as the full experiential design of the experiment and the Taguchi method [14]. The whole factory method is more convenient to improve the process. The method of Taguchi cannot detect the effects of reaction in this process [15]. The drawing approach corresponds to the requirements of both optimization and modeling needs. It uses computational and statistical techniques to represent the range of all possible solutions to the process model [9]. It is the best method for the empirical study of the relationships between one or more measured response function. The work has been focused on drawing by Zhao, et al., [16] on microelectronics applications, and examines transparency and resistance to film thin film properties. In the development of coating processes, understanding factors that affect the performance of coatings are imperative. That the three main factors that significantly affect the properties of the paint performance is: particle bombardment of film growing, substrate temperature, and Composition of elements in coatings. This research focuses on ionic bombardment and temperature effects only. Since the ion bombardment is affected by process parameters and the substrate temperature is also one of the parameters of the BID process, the modeling work will only focus on these process parameters as input variables to the model. The aim of this study is to check the effect of substrate bias voltage, argon gas pressure and sputtering power on the crystalline grain Size and microstructure of deposition coating using a surface response methodology (RSM). This comprehensive approach to evaluating the behavior of PVD process is few in previous research.

2. Design the Experiment

The experiment was run in unbalanced PVD magnetron sputtering system made of VACTEC Korean model VTC PVD 1000 which has two vertically mounted AlTi alloys. This system also consists of the substrate holder with adjustable planetary rotation. Figure 1 (a) shows the PVD magnetron sputtering system. The titanium alloy was selected as the target material and the chemical compositions of the material was 50% of titanium and 50% of aluminum. The surface of tungsten carbide (WC specimen) cutting tool insert was cleaned with alcohol bath in an ultrasonic cleaner for 20 minutes as shown in Figure 1 (b). The substrates were loaded into the rotating substrate holder inside the coating chamber. The rotation speed was set at 5 rpm. Argon gas was used to produce electron and sputter the target material. The substrate was coated with the alloy in the presence of nitrogen gas as the reactive gas. The experimental matrix and data analysis were based on the design of an RSM center cubic design, using the expert design software version 7.0.3. It included 8 factorial points, 4 axial points and 6 central points to enable the estimation of process fluctuations as shown in **Figure 3**.

(a) (b)

Figure 1: (a) PVD unbalanced magnetron sputtering system model VTC PVD 1000, and (b) ultrasonic bath cleaner

Table 1: Factors and levels selected for the experiments

	Ar gas pressure mbar	**Sputtering power kw**	**Bias voltage V**
- Alpha	3.0 x 10^{-3} mbar	4.000	50
+ Alpha	5.0 x 10^{-3} mbar	8.000	300

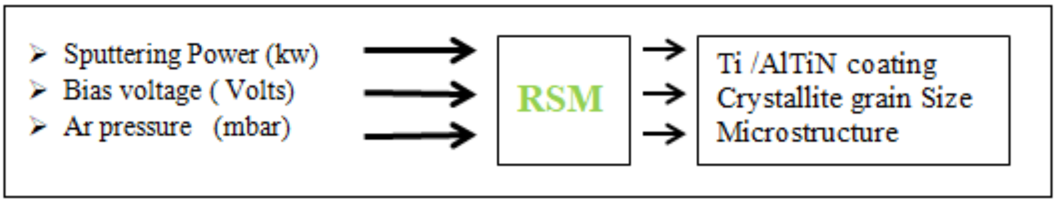

Figure 2: The inputs and output of the RSM model.

The experimental matrix was designed based on the determination of maximum points (operating window) as +/- alpha value, to the specified extreme point values, the program determines the high and low settings of standard points. This was to ensure that the characterization can be performed covering the widest possible range of the operating window of the relevant parameters. Because of this, the value of the reference points was not well rounded. The advanced experimental matrix is drawn on the basis of the composite central design, and the alpha +/- values specified in Table 1, 2, as shown in Figure 3. A CCD consists have three of design points: A two level factorial design points and axial points: The axial points have all of the factors are set to 0, the midpoint, except one factor, which has the value +/- Alpha. The value of Alpha is calculated in each design for both orthogonality and rotatability of blocks (6 points). Addition center points: Center points were repeated 6 times to get a good estimate of experimental error (pure error). The experimental research study matrix was designed based on specify the extreme points for an operating window function as the +/- Alpha value, shown as

Table 2. Based on the defined predicate in a proposition point value, the software then assigned the high and low settings for the factorial points. Extent indicated this was to ensure the modelling could be performed covering the widest range of operating window possible for respective parameters.

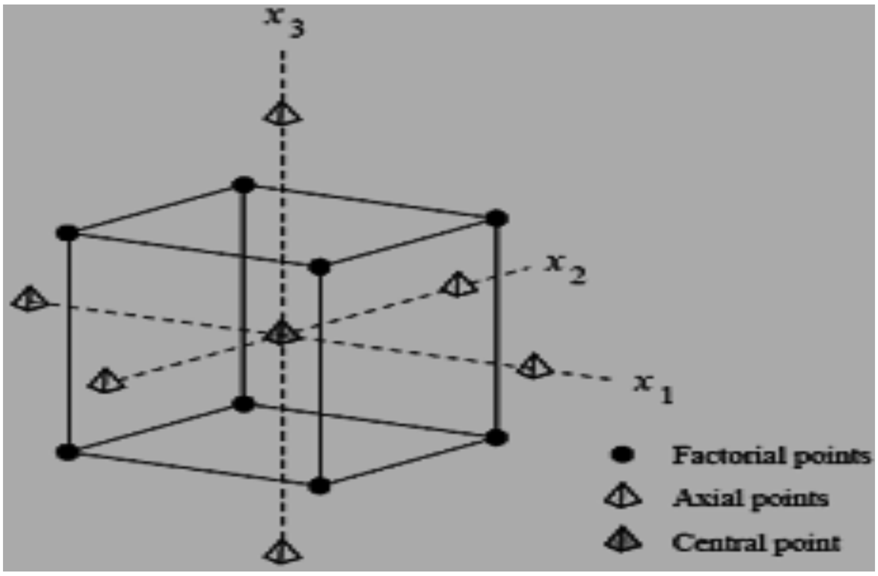

Figure 3: RSM Central Composite Design for 3 factors at two levels

Because of this the values of factorial points were not perfectly rounded surface. The experimental matrix ahead developed based on the RSM central composite design and the +/- Alpha values defined in Table 2**,** as shown in Figure 4 and 5. The run consisted of each experimental three samples and the sequence of experiment things follow each other the randomly assigned run number as reflected in Table 2. Surface roughness analysis and microstructure were performed following this series of steps. Figure 5 shows typical two-dimensional AFM morphology images of the Ti/AlTiN coatings deposited at of thickness layer 2.717µm to 8.760µm. The measured area of 10x10 µm2 was selected for the random position of the coatings. Schematic Thornton structure zone diagram shows beyond doubt the dependent of coating structure of substrate temperature and argon pressure. Addition, note that we did not take the temperature into account in this research as show in Figure 4 schematic Thornton structure zone diagram while work focus only argon gas.

3. Results and Discussion

The twenty specimens experiment on basis data and roughness are organized in the following table as shown below in the Table 2.

Table 2: The various stages in processing the modelling experimental matrix for PVD process on RSM central composite design approach

Run Order	Ar gas pressure	Bias voltage	Sputtering power	Roughness
	mbar	***v***	***KW***	***(µm)***
1	0.00459	249.33	4.810	0.07157
2	0.00459	100.67	4.810	0.08855
3	0.00400	50.00	6.000	0.09868
4	0.00341	100.67	4.810	0.19439
5	0.00400	175.00	4.000	0.19060
6	0.00400	175.00	6.000	0.2580
7	0.00400	175.00	6.000	0.1487
8	0.00341	100.67	7.190	0.1602
9	0.00459	249.33	7.190	0.2861

10	0.00400	175.00	6.000	0.3010
11	0.00400	175.00	6.000	0.3586
12	0.00400	300.00	6.000	0.3909
13	0.00400	175.00	6.000	0.4293
14	0.00341	249.325	4.810	0.4684
15	0.00400	175.000	8.000	0.5236
16	0.00459	100.67	7.190	0.5957
17	0.00300	175.00	6.000	0.6143
18	0.00500	175.00	6.000	0.6835
19	0.00341	249.33	7.190	0.7091
20	0.00400	175.00	6.000	0.7856

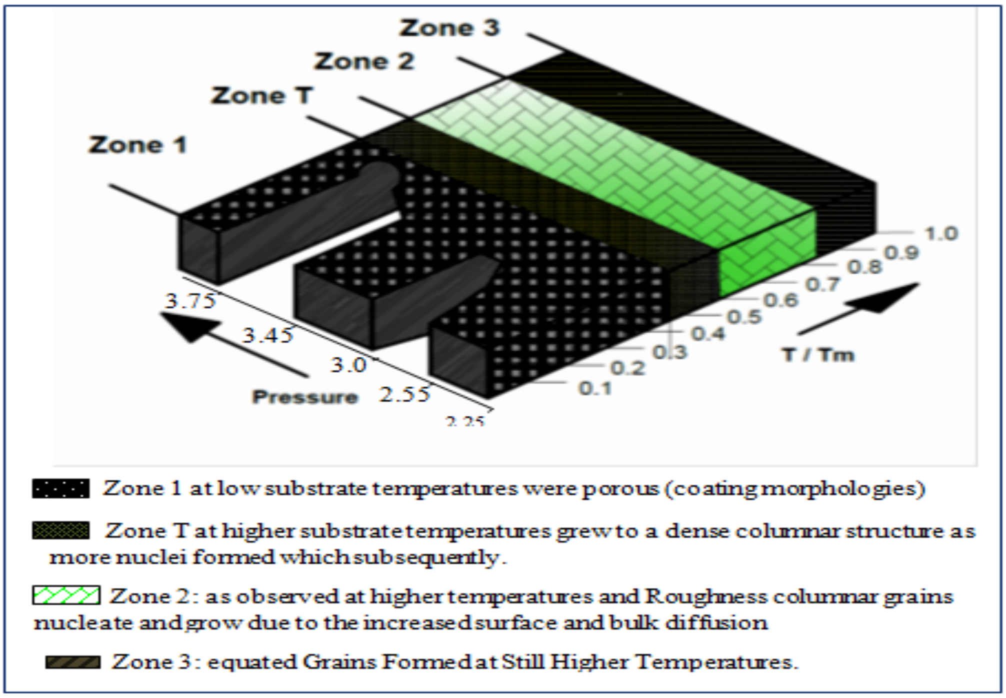

Figure 4: Schematic Thornton structure zone diagram showing the dependence of coating structure on substrate temperature and argon pressure

4. Atomic Force Microscopy (AFM):

A device atomic force microscopy (AFM) was used to examine and analyze the roughness of the surface for only five samples (WC) from the 20 for it is difficult to solution to understand description for all samples. So that we can determine the roughness then of the detection mode using a mode commercial Si3N4 cantilever and the scanning area was set at 10x10 μm^2. These surfaces of the samples indicate the differences according to the conditions of the completed shown in **Figure 5.**

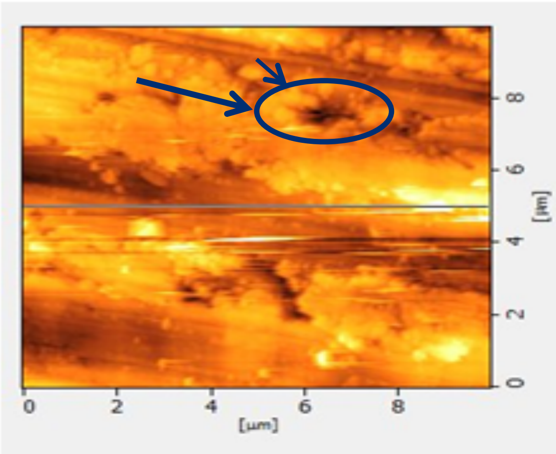

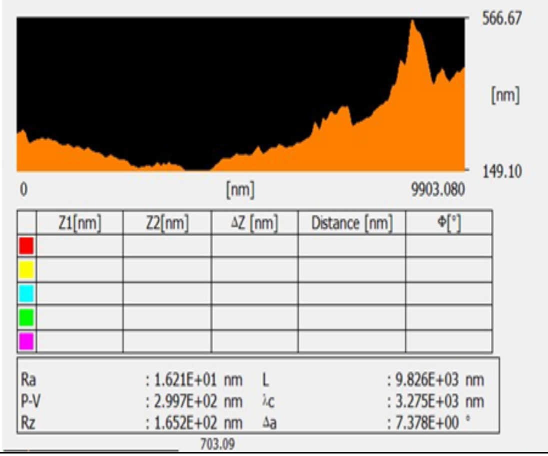

(a): Thickness 2.717μm boundary line with subdued finer grains.

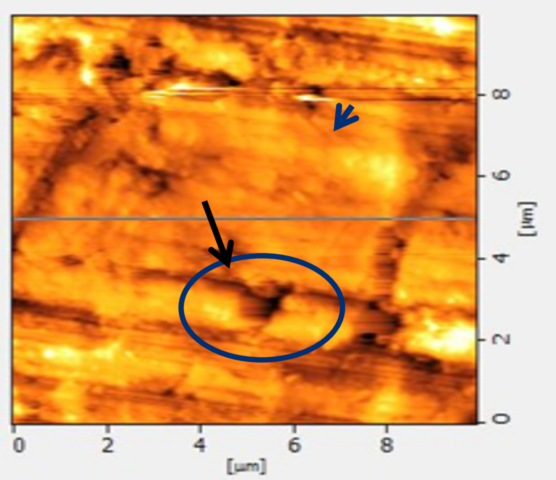

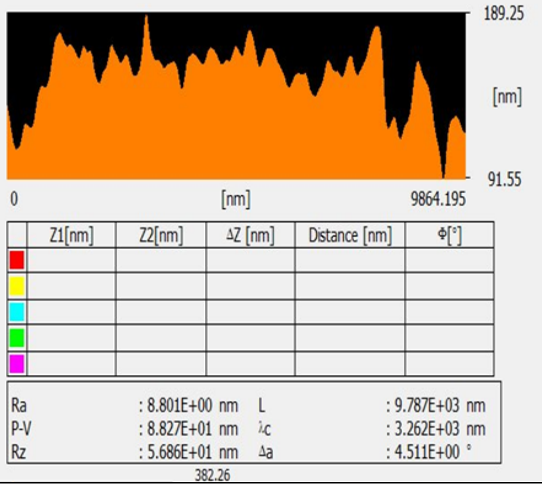

(b): Thickness 3.089μm Argon bombardment weak for ions of may be the reason for light lines and produce (a hole) on a surface.

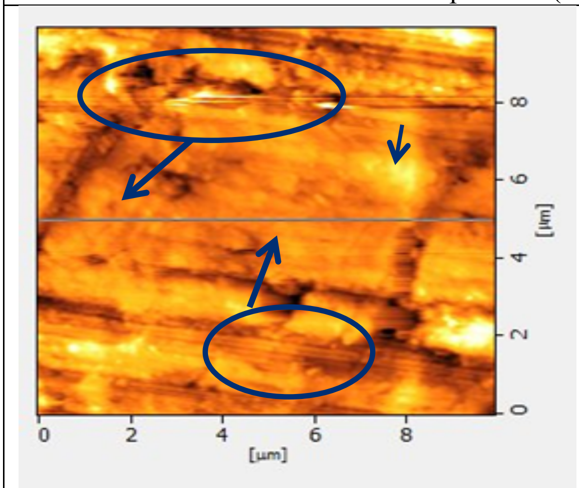

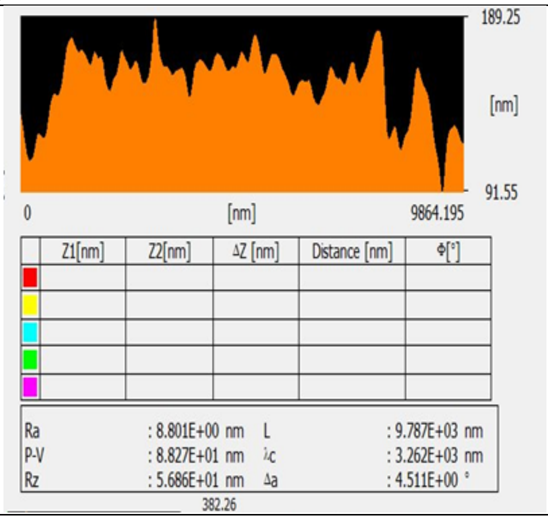

(c): Thickness 3.912μm, Behavior of the coating roughness relation to interaction between sputtering power and argon gas pressure

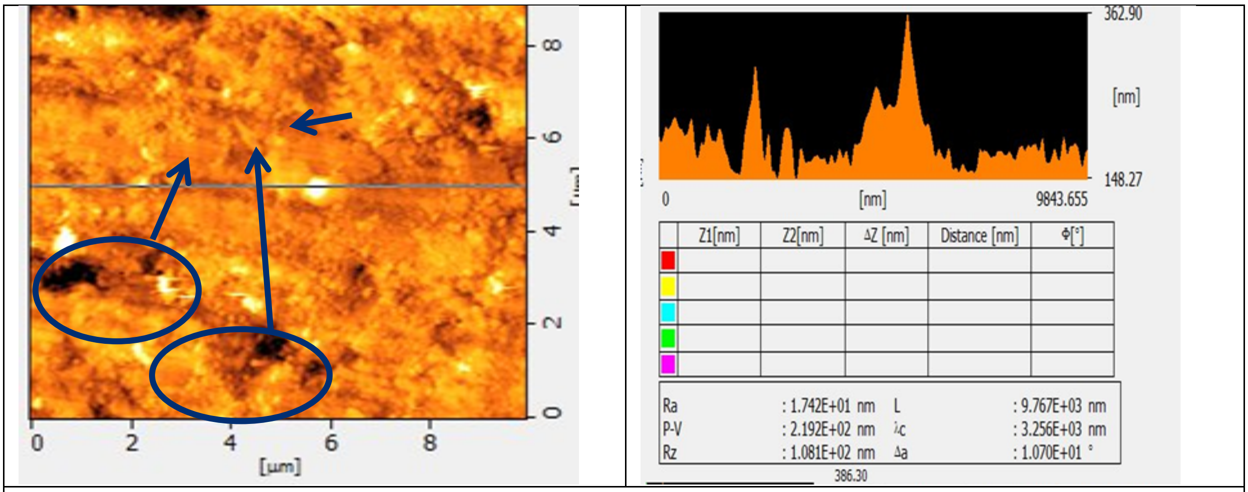

(d): Thickness 5.815µm, Affects coating characteristics and crystalline grain size

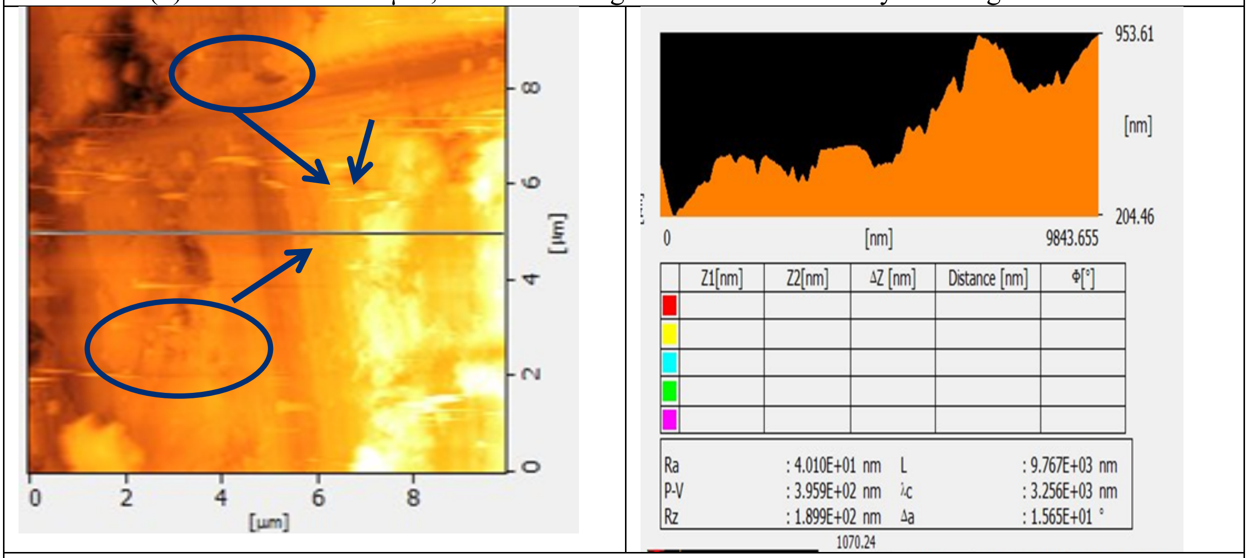

(e): Thickness 8.760818µm, Bias voltage affects coating characteristics and surface roughness, crystalline size, and porous, the decrease in grain size can be attributed to higher numbers and greater energy of the depositing atoms onto the substrate surface.

Figure 5: Two dimensional AFM image of tungsten carbide; a =2.717µm; b =3.089µm; c =3.912µm; d =5.815µm; e =8.760818µm surface various thicknesses with layer (AlTiN) coating; caption 10 x 10 microns (100µm2).

Significant factors affecting coating roughness and interactions on surface roughness were determined by conducting ANOVA analysis of experimental data. The ANOVA analysis is shown in Table 3. Based on the P value below 0.050, it is learned that the sputtering power, the interaction between the sputtering power and the gas pressure, and the substrate bias are significant factors of the resulting surface roughness. The "Model F-value" of 0.45 strongly suggest the truth or existence, of implies the model is not significant relative to the noise. There is an 89.28 % opportunity that a "Model F-value this relatively great size could occur due to noise. Values of "Prob > F" less than 0.0500 indicates model terms are significant. In this case there are no significant model terms. Values greater than 0.1000 indicate the model terms are not significant. If there are many insignificant model terms (not counting those required to support hierarchy), model reduction may improve your model. The "Lack of Fit F-value" of 2.75 implies the Lack of Fit is not significant relative to the pure error. There is a 15.84% chance that a "Lack of Fit F-value" this large could occur due to noise. Nonsignificant lack of fit is good -- we want the model to fit. Table 3:

Table 3: Analysis of variance (ANOVA) for RSM quadratic Model.

Source	**Sum of Squares**	**df**	**Mean Square**	**F Value**	**p-value Prob > F**
model	0.47	13	0.036	0.45	0.8928
A-Argon Pressure	0.20	4	0.050	0.62	0.6623
B-Sputtering Power	1.634E-003	1	1.634E-003	0.020	0.8915
C-Bias Voltage	0.064	1	0.064	0.80	0.4059
AB	0.027	2	0.014	0.17	0.8497
AC	0.086	2	0.043	0.53	0.6126
BC	0.030	1	0.030	0.37	0.5652
B^2	0.11	1	0.11	1.41	0.2794
C^2	0.039	1	0.039	0.49	0.5109
Residual	0.48	6	0.081		
Lack of Fit	0.17	1	0.17	2.75	0.1584
Pure Error	0.31	5	0.063		
Cor Total	0.96	19			

Discussion, suggestion as to a possible idea, on the influence of sputtering power, interaction between sputtering power and argon gas pressure, and substrate bias quadratic term are as the following:

5. Sputtering powers:

As the argon pressure increases from 4 kW to 8 kW, coating roughness reduced from 0.00231821mbar to 0.005681mbar (Figure 6). This is aligned with the findings by kamil. J. [2] who have reported a decrease in roughness with the increase in gas argon pressure. But unevenly up and down so that, she was internal plasma a weak room coating adds to bias voltages. The decrease in grain size can be attributed to higher numbers and greater energy of the depositing atoms onto the substrate surface. This condition is more favorable for the nucleation of new grains than the growth of existing ones.

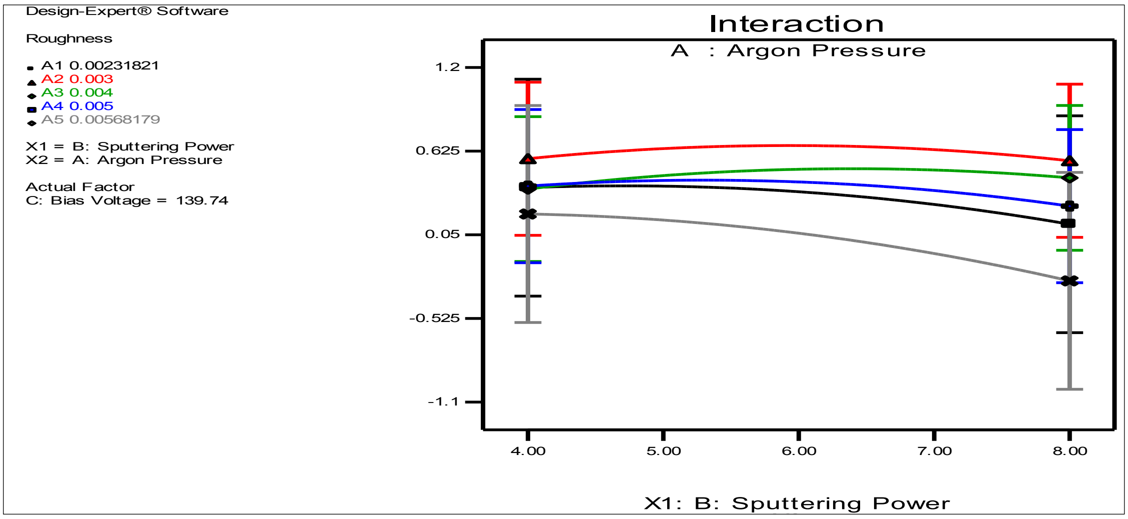

Figure 6: Behavior of coating roughness in response to sputtering power.

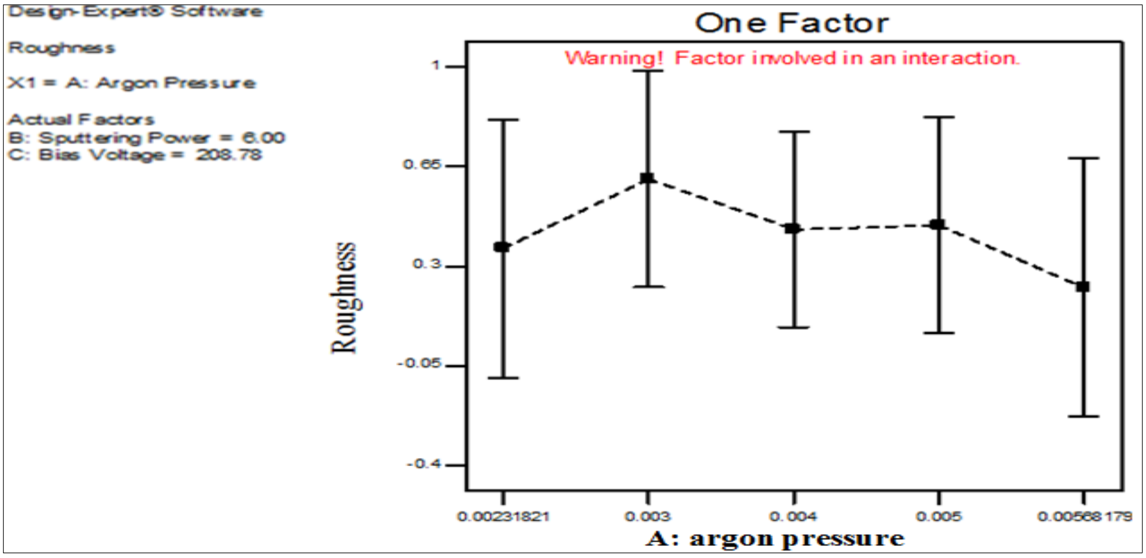

Figure 7: Behavior of coating roughness relative to interaction between sputtering power and gas argon pressure.

Behavior of the coating roughness relation to interaction between sputtering power and argon gas pressure. The instability of argon gas internally the coating chamber effect of an action of an expression which is involving one or more variable or other cause of the presence of this defect therefore, the interaction of effect between bias voltage and argon pressure as shown in Figure 7, gives a clearer and detailed picture.

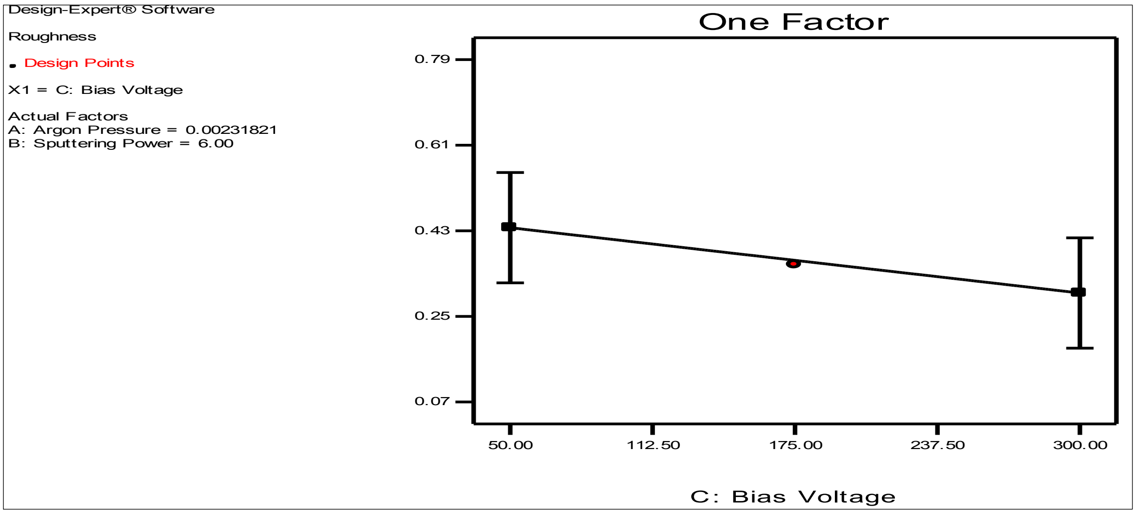

Figure 8: Behavior of coating roughness as a function of substrate bias voltage.

As give a long process involving a great deal of careful consideration to in Figure. 8, as the substrate bias increases from 50 to 175 V the coating roughness decrease from 0.43 µm to 0.36 µm. Meanwhile, as the substrate bias increases from 175V to 300 V, the coating roughness increases from 0.36 µm to 0.29 µm. This quadratic behavior can also be inferred from the ANOVA analysis in Table 2 and Table 3 where the quadratic characterize of substrate bias is one of the significant terms that influence coating roughness. From these facts we can infer that roughness has been increasing. This finding is aligned with discussion and research by Nizam et al., which have indicated that as the substrate bias increased from 0 V to 200V, the developed coating roughness reduced significantly. The upward trend of coating roughness beyond a certain substrate bias level, as indicated in this study, was also reported by kamil et al. [2]. This could be due to imperfection of coating surface caused by bombardment of ions with an excessively high energy level above certain substrate bias voltage (B. Deng et al. 2012). Figure 5 (a - e), shown in fitted detail provided with each specific and component part via the AFM images provide visual evidence of the reduction of grain size and smoother surface morphology of the Ti/AlTiN coating as the substrate bias voltage increases and the respective SEM images of the fractured cross section indicates a reduction in porosity and the formation of a dense columnar structure at higher bias voltage as shown in Figure 4. The reduction in grain size can be attributed to the increase in ion bombardment as a result from substrate bias incremental changes. This is due to higher nucleation density resulting in fine-grained morphology [17]. Consequent to due to ion bombardment the energy impacted upon the growing coating, as well assistance to anneal out flaws in the coating. Figure 5 (c), proven this, as the substrate bias was further increased to 300V, flaws of coating morphology occurred possibly due to re-sputtering of the deposited coating. Adding these it, with embedded refer to AFM image and scanning electron microscopy (SEM) image indicating the transformation of grain size and morphology of the Ti/TiAlN coating as the substrate bias increases.

6. Conclusion:

Achieving results to used PVD sputtering process at different levels during Ti/AlTiN coatings were deposited and employed substrate gas argon pressure, substrate bias voltages, and substrate sputtering powers following the experimental matrix developed, based on RSM approach. The action findings of this have indicated that sputtering power, interaction between substrate argon gas, sputtering power and substrate bias quadratic term are the significant process parameters that influence the deposited TiAlN coating roughness. The decrease in surface roughness due to finer grain size formation resultant for increment, in sputtering power. In the course of this, through reciprocal action and the interaction between sputtering power and argon gas have indicated that at lower substrate argon gas for various reasons, and lower substrate temperature level the change in sputtering power resulted in insignificant changes in coating roughness attributed to the suppressed preferential crystal growth which resulted in smoother surfaces. The substrate bias voltage has an influence on coating roughness in a quadratic behavior where an increase in substrate bias voltage up to 175V resulted in lower roughness value; however, increment beyond that value resulted in higher surface roughness.

Reference

[1] Y. Birol, and D. Isler. (2010). "AlTiN and AlTiON-coated hot work tool steels for tooling in steel thixoforming", *Trans. Nonferrous Met. Soc.* China 20s1022-s1028

[2] Kamil J. Kadhim, Nizam Abd Rahman, Mohd Rizal Salleh, and Khairul Izani Mohd Zukee., (2015). Effects of Layer Thickness on the Microstructures of TiN/AlTiN Multilayer *Coatings Applied Mechanics and Materials* Vol. 761: pp 417-420

[3] Xin Wang, Parick Y. Kwon, David Schrock, Dave (Dae-Wook) Kim. (2013). Friction coefficient and sliding wear of AlTiN coating under various lubrication conditions, *Wear* 304: 67–76.

[4] C.X. Tian, B. Yang, S.J. Yan, Z.H. Lu, Z.H. Huang, D.J. Fu., (2013. Influence of substrate rotation speed on the structure and mechanical properties of AlTiN/CrN coatings, *Surface & Coatings Technology* 228: S228–S232

[5] Liu Aihua, Deng Jianxin, Cui Haibing, Chen Yangyang, Zhao Jun., (2012). Friction and wear properties of TiN, TiAlN, AlTiN and CrAlN PVD nitride coatings. *Int. Journal of Refractory Metals and Hard Materials* 31: 82–88

[6] Y.H. Zhao, L. Hu, G.Q. Lin, J.Q. Xiao, C. Dong, and B.H. Yu., (2012). Deposition, microstructure and hardness of TiN/(Ti,Al)N multilayer films, *Int. Journal of Refractory Metals and Hard Materials* 32: 27–32

[7] Caiceiro, J. C., Cabrera, G., Caiceido, H. H., Amaya, C., and Aperador, W., (2012). Nature in corrosion-erosion surface for [TiN/TiAlN] n nanometric multilayers growth on AISI 1045 steel, *Thin Solid Films* 520 4350-4361.

[8] P. Panjan, P. Gselman, D. Kek-Merl, M. Čekada, M.Panjan ,G.Dražić ,T. Bončina, F.Zupanič ., (2013). Growth defect density in PVD hard coatings prepared by different deposition techniques, *Surface & Coatings Technology* xxx: xxx–xxx

[9] D. Kottfera, M. Ferdinandy, L. Kaczmarek, I. Maˇ nková, and J. Bnoa., (2013). Investigation of Ti and Cr based PVD coatings deposited onto HSS Co 5twist drills, *Applied Surface Science* 282 :770– 776

[10] B. Warcholinski, and A. Gilewicz., (2011). Multilayer coatings on tools for woodworking, *Wear* 271: 2812– 2820

[11] Abdul Syukor Mohamad Jaya, Abd Samad Hasan Basari, Siti Zaiton Mohd Hashim, Habibollah Haron, Muhd. Razali Muhamad and Md. Nizam Abd. Rahman, (2011). Application of ANFIS in Predicting of TiAlN Coatings Hardness, *Australian Journal of Basic and Applied Sciences*, 5(9): 1647-1657.

[12] Dagmar Jakubéczyová, Maria Hagarová, Ivo Stepanek., (2011). Evaluation of Thin PVD Coatings, Annals of Faculty Hunedoara – *International Journal of Engineering*, Tome IX. Fascicule 1.

[13] B. Podgornik, B. Zajec, N. Bay, J. Vižintin., (2011). Application of hard coatings for blanking and piercing tools, *Wear* 270 850–856.

[14] Yun-Kon Joo, Shi-Hong Zhang *, Jae-Hong Yoon and Tong-Yul Cho.,2009. "Optimization of the Adhesion Strength of Arc Ion Plating TiAlN Films by the Taguchi Method" *Materials* 2009, 2, 699-709.

[15] A.I. Kovalev, D.L. Wainstein, A.Y. Rashkovskiy, G.S. Fox-Rabinovich, K. Yamamoto, S. Veldhuis, M. Aguirre, and B.D. Beake., (2010). Impact of Al and Cr alloying in TiN-based PVD coatings on cutting performance during machining of hard to cut materials, *Vacuum* 84 184–187.

[16] Yanhui Zhao, Guoqiang Lin, Jinquan Xiao, Chuang Dong, Lishi Wen., (2010). TiN/TiC multilayer films deposited by pulse biased arc ion plating, *Vacuum* 85 1–4

[17] L. A. Dobrzanski, M. Staszuk, K. Golombek, A. Sliwa, M. and Pancielejko. (2010). Structure and Properties PVD and CVD Coatings Deposited onto Edges of Sintered Cutting Tools, *Archives of Metallurgy and Materials*, vol. 55 (1) 187-193.